DOI: *http://dx.doi.org/10.18502/cjn.v24i2.20693*

Current Journal of Neurology

Review Paper

Curr J Neurol 2025; 24(2): 168-76

Systematic review of curcumin-based optical imaging for amyloid-β detection in Alzheimer's disease models

Received: 25 Nov. 2024
Accepted: 03 Feb. 2025

Kimia Safavian[1], Mohsen Cheki[2], Sahel Heydarheydari[2]

[1] Student Research Committee, Ahvaz Jundishapur University of Medical Sciences, Ahvaz, Iran
[2] Department of Medical Imaging and Radiation Sciences, School of Paramedicine, Ahvaz Jundishapur University of Medical Sciences, Ahvaz, Iran

Keywords
Alzheimer's Disease; Amyloid-Beta; Optical Imaging; Curcumin; Fluorescent Probes; Preclinical

Abstract

Background: Alzheimer's disease (AD) is a neurodegenerative disorder characterized by amyloid-beta (Aβ) plaque accumulation and cognitive decline. Early and precise Aβ detection is vital for effective therapeutic intervention. Curcumin-based fluorescent probes offer high specificity, non-invasive imaging compatibility, and deep tissue penetration, making them promising tools for optical Aβ imaging. This systematic review evaluates preclinical studies on curcumin-based fluorescent probes to assess their photophysical properties, imaging capabilities, and potential applications in detecting Aβ plaques in mouse models of AD.

Methods: A comprehensive literature search was performed in PubMed and ScienceDirect (2000-2024). Eligible studies were original English-language articles using curcumin-based probes for optical imaging of Aβ in Alzheimer's mouse models. Data extraction focused on imaging parameters such as binding affinity [dissociation constant (Kd)], emission wavelength, quantum yield, fluorescence enhancement, and delivery methods.

Results: Thirteen preclinical studies met the inclusion criteria and were analyzed. CRANAD-102 probe showed the highest binding affinity (Kd = 7.5 nM) while CRANAD-3 achieved the most significant fluorescence intensity (39.5-fold). Emission wavelengths averaged 690 nm, with longer wavelengths facilitating deeper tissue imaging. Quantum yields ranged from 0.011 to 0.40, with the highest yield (20.31) observed in CH_2Cl_2 and effective doses averaging 2.0 mg/kg.

How to cite this article: Safavian K, Cheki M, Heydarheydari S. Systematic review of curcumin-based optical imaging for amyloid-β detection in Alzheimer's disease models. Curr J Neurol 2025; 24(2): 168-76.

Corresponding Author 1: Mohsen Cheki
Email: mohsencheky@gmail.com
Corresponding Author 2: Sahel Heydarheydari
Email: sheydari7@gmail.com

Innovative delivery methods, such as aerosolized formulations and micelle-based probes, expanded diagnostic applications, including non-invasive retinal imaging.

Conclusion: Curcumin-based fluorescent probes exhibit high specificity for Aβ aggregates, effective deep tissue imaging, and non-invasive delivery potential, making them promising tools for preclinical Alzheimer's diagnostics. However, their clinical translation requires further validation in standardized preclinical and translational studies.

Introduction

Alzheimer's disease (AD) is a progressive neurodegenerative disorder marked by cognitive decline, memory loss, and behavioral dysfunction, predominantly affecting the elderly. As the global population ages, AD poses a growing burden due to increasing rates of disability and mortality.[1-3] Despite advances in symptomatic treatment, no curative therapy exists, making early and accurate diagnosis essential for timely intervention and slowing disease progression.

One of the earliest pathological hallmarks of AD is the extracellular accumulation of amyloid-beta (Aβ) plaques, formed through aberrant cleavage of amyloid precursor protein (APP) by β- and γ-secretases. Notably, this accumulation begins up to two decades before clinical symptoms emerge,[4] highlighting the critical need for sensitive, non-invasive, and scalable diagnostic tools capable of detecting Aβ pathology in the preclinical stages.

Conventional imaging modalities such as positron emission tomography (PET), single-photon emission computed tomography (SPECT), and magnetic resonance imaging (MRI) have been employed to visualize Aβ burden. However, these approaches are limited by high cost, radiation exposure, limited accessibility, and technical complexity.[1] Optical imaging, particularly using near-infrared (NIR) fluorescence probes, offers several advantages including non-invasiveness, high sensitivity, real-time imaging capability, and cost-effectiveness. Ideal NIR probes for Aβ detection must exhibit high specificity, strong quantum yield, appropriate lipophilicity, long-wavelength emission (> 650 nm), and minimal off-target interactions.[5,6]

Curcumin, a natural polyphenol from Curcuma longa, has emerged as a promising scaffold for Aβ-targeting fluorescent probes due to its ability to cross the blood-brain barrier (BBB), bind β-sheet-rich Aβ aggregates, and emit in the visible to NIR range. Numerous curcumin derivatives have been developed to overcome limitations such as poor bioavailability and rapid metabolism, with several demonstrating success in detecting Aβ plaques in the brain and retina of transgenic (Tg) AD mouse models.[7]

Despite promising preclinical data, the clinical translation of curcumin-based probes remains limited. Challenges include species-specific pharmacokinetics, variability in fluorescence performance across formulations, and lack of regulatory standardization. Nonetheless, these probes offer a strong foundation for the design of cost-effective, non-radioactive, and early diagnostic tools for AD. To address this translational gap, the present systematic review synthesizes preclinical evidence on curcumin-based fluorescent probes for Aβ imaging. Specifically, we aim to characterize their photophysical properties, imaging performance, and delivery strategies in Tg AD mouse models.

To our knowledge, this is the first systematic review to integrate photophysical characteristics, in vivo imaging outcomes, and delivery strategies of curcumin-based probes in Tg AD mouse models. Unlike previous reviews, our work provides a comparative synthesis focused on probe structure-function relationships and their in vivo applicability, offering practical insights for the rational design of next-generation diagnostic agents. This review highlights how curcumin derivatives may inform future probe selection and contribute to the refinement of in vivo imaging technologies for early AD diagnosis.

Materials and Methods

This systematic review followed the Preferred Reporting Items for Systematic Reviews and Meta-Analyses (PRISMA) 2020 guidelines to ensure methodological transparency and reporting completeness.

Search strategy: A systematic literature search was conducted using two major biomedical databases – PubMed and ScienceDirect – to identify relevant preclinical studies published between January 2000 and March 2024. In addition to database queries, Google Scholar citation tracking tools were used to identify further eligible studies through backward and forward reference searching. This approach was employed to enhance the breadth of the review by capturing relevant publications that may have been indexed

in other platforms.

The search strategy incorporated a combination of Medical Subject Headings (MeSH) and free-text keywords to ensure comprehensive coverage. The primary search terms included: "Alzheimer Disease" (MeSH) OR "Alzheimer's", "Amyloid beta-Peptides" (MeSH) OR "amyloid-β" OR "Aβ", "Curcumin" (MeSH), and "Optical Imaging" (MeSH) OR "fluorescence imaging". Boolean operators (AND, OR) were applied systematically to combine these terms and optimize retrieval sensitivity and specificity.

The search was restricted to original, peer-reviewed articles published in English during the specified period. Only full-text articles were included, while reviews, editorials, conference abstracts, and studies without accessible full texts were excluded.

The complete search strategy is provided in table 1, and the overall article selection process is depicted in figure 1.

Selection criteria: Articles were screened for relevance based on their titles and abstracts. The extracted data from the title and abstract had to meet the following criteria:

1) The study utilized optical imaging to evaluate and identify bilateral AD,

2) Curcumin was employed as a fluorescent probe for detecting Aβ,

3) The research was conducted using an animal model (mice).

Inclusion and exclusion criteria

Studies were included if they:

1) Utilized mouse models of AD,

2) Employed fluorescent imaging techniques for the detection of Aβ plaques.

Studies were excluded if they:

1) Were reviews or non-original research,

2) Did not provide full-text access.

Data extraction and analysis: Full-text articles were thoroughly reviewed, and studies that did not address the research question or provided insufficient data were excluded. No studies were excluded due to marginal eligibility; all exclusions were based on clearly defined criteria during full-text screening.

Ultimately, 13 studies were selected for analysis based on their focus on optical imaging in animal models of AD and their exploration of curcumin's effects on Aβ.

Outcomes and variables of interest: The primary outcomes extracted from each study included: (1) binding affinity to Aβ aggregates [expressed as dissociation constant (Kd)], (2) quantum yield of fluorescence, (3) emission wavelength (λmax), (4) fluorescence signal enhancement, and (5) effective dose in mg/kg.

Additional variables extracted included: (1) physicochemical properties such as partition coefficient (logP), (2) delivery methods [e.g., intravenous (IV) injection, aerosol, micelle-based formulation], (3) cytotoxicity profiles, and (4) imaging targets such as brain cortex or retina. In cases where specific values were not reported, no assumptions were made, and such fields were documented as "not available (NA)".

Effect measures: For each included study, the primary effect measures extracted were:

1) Kd (in nM) to reflect probe binding affinity to Aβ,

2) Fluorescence signal enhancement ratios [e.g., fold-change vs. control or wild-type (WT)],

3) Emission wavelength (λmax, in nm) as a measure of optical penetration potential, and

4) Quantum yield as an indicator of fluorescence efficiency.

These metrics were used to qualitatively and quantitatively compare the performance of different curcumin-based probes across studies.

Table 1. Search strategy

	Search strategy
Databases	PubMed, ScienceDirect
Time frame	January 2000-March 2024
Keywords and MeSH terms used	("Alzheimer Disease"[MeSH Terms] OR "Alzheimer"[All Fields] OR "Alzheimer*"[All Fields]) AND ("Amyloid beta-Peptides"[MeSH Terms] OR "amyloid-beta"[All Fields] OR "amyloid-β"[All Fields] OR "Aβ"[All Fields]) AND ("Curcumin"[MeSH Terms] OR "curcumin"[All Fields]) AND ("Optical Imaging"[MeSH Terms] OR "optical imaging"[All Fields] OR "fluorescence imaging"[All Fields])
Search methodology	Boolean operators (AND, OR) were systematically applied to combine the search terms and ensure both sensitivity and specificity in retrieval. Filters were applied to include only peer-reviewed original articles published in English between 2000 and 2024. Additionally, citation tracking (both backward and forward) was used to identify further relevant studies through reference lists of included articles.

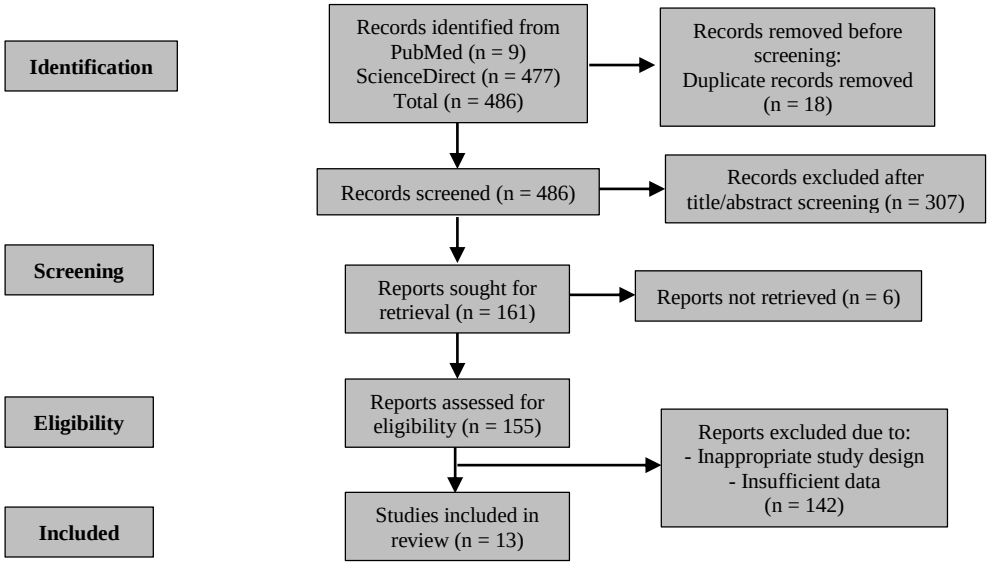

Figure 1. Preferred Reporting Items for Systematic Reviews and Meta-Analyses (PRISMA) flowchart summarizing the search strategy and study selection process

Data preparation: No data conversions or transformations were required, as all relevant outcomes were directly reported in the included studies.

Synthesis of results: A narrative synthesis approach was employed to compare and interpret findings across studies. No statistical pooling or meta-analysis was performed. No subgroup analysis or formal assessment of heterogeneity was conducted, as the review was not designed for quantitative synthesis. Sensitivity analyses were not applicable given the descriptive nature of the synthesis.

Quality assessment: To ensure methodological rigor and transparency, the risk of bias for each included preclinical study was systematically assessed using SYRCLE's Risk of Bias Tool, a domain-based instrument specifically developed for animal research. The assessment covered five key domains: (1) random sequence generation (selection bias), (2) allocation concealment (selection bias), (3) blinding of investigators and outcome assessors (performance and detection bias), (4) completeness of outcome data (attrition bias), and (5) selective outcome reporting (reporting bias).

Two independent reviewers conducted the assessments, and any disagreements were resolved through discussion and consensus. Risk of bias judgments were applied across all included studies and summarized narratively in the manuscript. Studies with a high overall risk of bias were excluded to ensure the internal validity of the findings.

No formal assessment of certainty or confidence in the body of evidence (e.g., using GRADE) was performed, given the descriptive nature of the synthesis.

Results

A total of 13 studies employing curcumin-based fluorescent probes for optical imaging of Aβ plaques in AD were reviewed. These studies evaluated photophysical properties, in vivo fluorescence measurements, and Aβ specificity in Tg mouse models. Key data are summarized in table 2.

Probe 9 (Fang et al.[2]) showed a 1.5-fold higher fluorescence intensity in APP/presenilin 1 (PS1) mice compared to WT [emission wavelengths: monomers = 690 nm, oligomers = 688 nm, aggregates = 697 nm; binding constants: monomers = 11.16 ± 0.79 nM, oligomers = 36.59 ± 2.69 nM, aggregates = 14.57 ± 1.27 nM; quantum yield = 20.31 (in CH_2Cl_2)]. Fluorescence signal increased with mouse age.

CAQ (Wu et al.[1]) in 5×FAD mice showed 1.57-fold higher fluorescence versus WT at 30 minutes post-injection (binding constant = 78.89 nM, logP = 3.08, quantum yield = 0.011).

Analog 8b (Park et al.[5]) exhibited 2.26-fold stronger fluorescence in 5×FAD mice versus WT at 10 minutes (emission λ = 667 nm, > 20-fold enhancement post-Aβ binding). Quantum yield was not reported.

Table 2. Summary of photophysical properties and fluorescence imaging characteristics of curcumin-based probes in the reviewed studies (Part I)

Study	Dose (mg/kg)	Quantum yield	LogP	Binding constant (Kd, nM)	Mouse model	Imaging technique
Wu et al.[1]	0.15	0.01	3.08	78.89	5×FAD Tg (10 months, female) WT (10 months, female)	- In vivo/ex vivo fluorescent imaging - FIHC
Fang et al.[2]	1.00	20.31 in CH_2Cl_2	2.14	Aβ oligomers: 36.59 ± 2.69 Aβ aggregates: 14.57 ± 1.27 Aβ monomers: 11.16 ± 0.79	APP/PS1 Tg (14 months, male) WT (14 months, male)	- In vitro fluorescent staining - In vivo NIRF imaging - Upright fluorescence microscopic imaging
Sidiqi et al.[3]	0.75	N/A	N/A	N/A	APP/PS1 Tg (6-18 months) WT (6-18 months)	-IHC -Whole-mount immunofluorescence - In vivo retinal fluorescence imaging with curcumin
Park et al.[5]	0.40	N/A	N/A	91.20 ± 3.28	5×FAD Tg (15 months, female) WT (15 months, female)	- In vivo NIRF imaging - Ex vivo and histological imaging
Ni et al.[6]	2.00	N/A	N/A	N/A	arcAβ Tg (18-24 months, both sexes) WT (18-24 months, both sexes)	- MSOT - Hybrid vMSOT-fluorescence imaging - MRI IHC
Si et al.[7]	3.00	0.37	N/A	1360.00	APP/PS1 Tg (17 months)	- In vivo NIRF imaging
Ran et al.[8]	5.00	0.40	3.00	38.00	2576 Tg (19 months) WT (19 months)	- Fluorescence intensity-based NIR imaging
Chibhabha et al.[9]	N/A	N/A	N/A	N/A	APPswe/PS1ΔE9 Tg C57BL	- Ex-vivo double immunofluorescence staining - In vivo imaging
Li et al.[10]	2.00	0.01	N/A	Soluble Aβ: 7.50 ± 10.00 Insoluble Aβ: 505.90 ± 275.90	APP/PS1 Tg (five months, female) WT (five months, female)	- In vivo NIRF imaging
Zhang et al.[11]	0.50	N/A	2.50	Aβ monomers: 24.00 ± 5.70 Dimers: 23.00 ± 1.60 Oligomers: 16.00 ± 6.70 Aggregates: 27.00 ± 15.80	APP/PS1 Tg (14 months, female) WT (14 months, female)	- Two-photon imaging - In vivo NIRF imaging
Zhang et al.[12]	2.00	N/A	1.94	Aβ40: 105.80 Aβ42: 45.80	APP/PS1 Tg (4 months, female) WT (4 months, female)	- In vivo NIR imaging
Koronyo-Hamaoui et al.[13]	7.50	N/A	N/A	N/A	APPswe/PS1ΔE9 Tg (18 months, female) WT (18 months, female)	- IHC - In vivo fluorescence imaging
McClure et al.[14]	5.00	N/A	N/A	N/A	5×FAD Tg (8 months) C57BL/6 WT (8 months)	- Ex vivo fluorescence brain imaging - IHC

Table 2. Summary of photophysical properties and fluorescence imaging characteristics of curcumin-based probes in the reviewed studies (Part II)

Study	Optical instrument	Emission wavelength	Probe	Brief result
Wu et al.[1]	- CLSM - Small animal live imager	726 nm in DMSO	CAQ	1.57-fold higher signal intensity in 5×FAD mice vs. WT at 30 minutes, strong binding to Aβ aggregates
Fang et al.[2]	- Leica TCS SP8 CLSM - Olympus VS200 microscope - IVIS Lumina XR III animal imaging system	Oligomers: 688 nm Aggregates: 697 nm Aβ Monomers: 690 nm	Probe 9	1.5-fold higher signal intensity in APP/PS1 mice vs. WT, strong Aβ affinity, low cytotoxicity
Sidiqi et al.[3]	- Confound fluorescent imaging - Fluorescence scanning laser ophthalmoscopy (fSLO)	N/A	Curcumin	Higher cortical and retinal Aβ signal intensity in Tg mice, correlating with cortical Aβ loads
Park et al.[5]	- Maestro 2.0 in vivo imaging system - CCD camera	λmax: 667 nm	8b curcumin analog	2.26-fold signal intensity enhancement in 5×FAD mice vs. WT at 10 minutes, high Aβ affinity, NIR emission
Ni et al.[6]	- Confocal microscope - A hybrid vMSOT-fluorescence imaging system	N/A	CRANAD-2	Dose-dependent signal intensity increase, significant AUC in cortical regions of arcAβ mice
Si et al.[7]	- IVIS Lumina system	λmax: 635 nm	Dye 2	Peak fluorescence 2 hours post-injection, high specificity for Aβ deposits, low cytotoxicity
Ran et al.[8]	- Fluorescence reflectance (also known as epifluorescence) and tomography (FMT)	λmax: 760 nm in methanol	CRANAD-2	Slower fluorescence decay in Tg2576 mice vs. WT, higher signal intensities at multiple time points
Chibhabha et al.[9]	- CLSM - Carl Zeiss LSM 780 - Micron IV retinal imaging microscope	N/A	DSPE-PEG2000 curcumin polymeric micelles	Labeled retinal Aβ plaques, robust deposition in retina and hippocampus, low toxicity
Li et al.[10]	- IVIS spectrum animal imaging system	N/A	CRANAD-102	1.22-fold higher signal intensity in APP/PS1 mice vs. WT at 30 minutes, selective for soluble Aβ species
Zhang et al.[11]	- IVIS spectrum animal imaging system	Around 730 nm	CRANAD-3	2.29-fold higher NIRF signal intensity in APP/PS1 mice vs. WT, effective across Aβ species and age groups
Zhang et al.[12]	- Spectrum animal imaging system - TEM	λmax ~ 750 nm	CRANAD-58	1.3-fold higher signal intensity in Tg mice vs. WT at 4 months, low off-target interactions
Koronyo-Hamaoui et al.[13]	- Micron II retinal imaging microscope - Carl Zeiss Axio Imager Z1 fluorescence microscope - Leica TCS SP5 double-spectral confocal microscope	N/A	Curcumin	Retinal Aβ signal intensity correlates with disease progression in Tg mice.
McClure et al.[14]	- Fluorescence tomographic imaging system - Dual channel fluorescence microscopy	N/A	FMeC1	FMeC1 binds amyloid plaques expressed in the hippocampal areas and cortex.

Data are presented as mean ± standard deviation (SD)

Kd: Dissociation constant; N/A: Not available; NIR: Near-infrared; Tg: Transgenic; WT: Wild-type; FIHC: Fluorescence immunohistochemistry; MSOT: Multispectral optoacoustic tomography; IHC: Immunohistochemistry; MRI: Magnetic resonance imaging; NIRF: Near-infrared fluorescence; TEM: Transmission electron microscopy; CLSM: Confocal laser scanning microscope; LSM: Laser scanning microscope; FMT: Fluorescence molecular tomography; CCD: Charge-coupled device; FMeC1: F-methyl-curcumin-1; APP/PS1: Amyloid precursor protein/presenilin 1; AUC: Area under the curve; Aβ: Amyloid-beta; vMSOT: Volumetric multispectral optoacoustic tomography; DMSO: Dimethyl sulfoxide

CRANAD-2 showed dose-dependent fluorescence for $A\beta_{1-42}$ fibrils ($r^2 = 0.991$). For $A\beta_{40}$ aggregates, fluorescence increased 70-fold (logP = 3.0).

CRANAD-102 had binding constants of 7.5 ± 10.0 nM (soluble Aβ) and 505.9 ± 275.9 nM (insoluble). In APP/PS1 mice, fluorescence was 1.22-fold higher than WT at 30 minutes.

1,2-distearoyl-sn-glycero-3-phosphoethanolamine-N-[methoxy(polyethylene glycol)-2000] (DSPE-PEG2000) (DSPE-PEG2000) micelles labeled retinal plaques; hemolytic activity was reported as 1.79%.

Dye 2 reached peak fluorescence at 2 hours post-injection (quantum yield = 0.37, cell viability > 85%).

CRANAD-3 showed 12.3-39.5-fold fluorescence increases across Aβ species (2.29-fold higher in APP/PS1 vs. WT, emission ≈ 730 nm).

CRANAD-58 (Zhang et al.[12]): Binding constants: $A\beta_{40}$ = 105.8 nM, $A\beta_{42}$ = 45.8 nM, logP = 1.94.

F-methyl-curcumin-1 (FMeC1) (McClure et al.[14]): Aerosol delivery targeted hippocampal/cortical plaques; fluorescence data were not quantified.

Other studies (Sidiqi et al.[3], Koronyo-Hamaoui et al.[13]) reported retinal and cortical fluorescence signals in Tg models, with retinal plaques detectable at ≥ 2.5 months.

Summary metrics

- Binding constants (Kd): Range = 7.5-1360 nM, mean ≈ 40.8 nM
- Quantum yields: Range = 0.011-20.31, mean ≈ 4.22. This observed variability is influenced by experimental factors such as solvent polarity, aggregation state of the probes, and the specific photophysical environment, which are not always standardized across studies.
- Emission wavelengths: Range = 635-760 nm, mean ≈ 690 nm
- Doses: Range = 0.15-7.5 mg/kg, mean ≈ 2.0 mg/kg

Noticeable variability may relate to solvent systems, probe aggregation, and delivery methods.

Risk of bias assessment: All studies were assessed using SYRCLE's Risk of Bias Tool. Domains related to random sequence generation, allocation concealment, random housing, and blinding were rated as "unclear" due to insufficient reporting. Remaining domains (baseline comparability, outcome completeness, selective reporting, and other biases) uniformly showed "low risk". No study was rated "high risk" in any domain.

Discussion

Developing non-invasive imaging tools for detecting Aβ deposits with high resolution is essential for understanding AD mechanisms and advancing Aβ-targeted therapies. Fluorescence imaging has been the primary application for most Aβ probes, including NIAD-4, AOI-987, boron-dipyrromethene (BODIPY), THK-265, Donor–acceptor near-infrared fluorophores (DANIR), luminescent conjugated oligothiophenes (LCOs), (E)-4-(4-(dibutylamino)styryl)-1-(2-hydroxyethyl quinolin-1-ium chloride (DBA-SLOH), and curcumin-derived CRANAD series.[2]

Curcumin, a natural compound capable of crossing the BBB, has shown promise in staining senile plaques and modulating amyloid pathology in Tg AD models. However, its use in NIR imaging has been limited by short emission wavelengths, low water solubility, poor BBB permeability, and rapid metabolic degradation. Strategies such as borate complexation have successfully induced red shifts in emission spectra, thereby improving imaging performance.[5]

This review highlights significant variability and complementarity among the studied curcumin-based fluorescent probes. CRANAD-102 exhibited the highest binding affinity for soluble Aβ species (Kd = 7.5 ± 10.0 nM), suggesting potential for detecting early pathological changes, whereas CAQ, despite lower affinity (Kd = 78.89 nM), offered advantages in safety and in vivo stability due to its low cytotoxicity and favorable logP (3.08).[1,10] In terms of fluorescence efficiency, probe 9 demonstrated the highest quantum yield (20.31 in CH_2Cl_2), supporting its use in high-signal imaging applications.[2] However, CRANAD-3 provided the broadest fluorescence enhancement (12.3-39.5-fold) across Aβ species and ages, and its NIR emission (~ 730 nm) made it suitable for deeper tissue imaging.[11] While analog 8b reached > 20-fold enhancement upon Aβ binding and performed well in rapid-onset models like 5×FAD mice,[5] CRANAD-2 stood out for its excellent BBB permeability (logP = 3.0) and dose-dependent signal increases.[6,8]

In terms of delivery and practicality, DSPE-PEG2000 micelle formulations improved solubility and biocompatibility, making them viable for retinal imaging,[9] while aerosolized FMeC1 enabled non-invasive midbrain imaging – an advantage over IV delivery routes.[14] These findings illustrate how specific probe modifications (e.g., red-shifting, polymeric encapsulation, or solubility enhancement) can optimize imaging for different diagnostic contexts,

from early detection to longitudinal monitoring.

Innovative delivery systems such as aerosolized curcumin derivatives and micelle-based formulations have expanded the diagnostic potential of these probes. FMeC1 delivered via aerosol enabled midbrain imaging without IV injection, while DSPE-PEG2000 micelles correlated well with retinal Aβ load, enabling non-invasive early diagnostics.[9,14]

Several studies also emphasized age-dependent imaging: retinal Aβ plaques were detectable as early as 2.5 months in Tg AD mice, aligning with early pathological events involving soluble Aβ species.[3] Importantly, variability in Tg mouse models may influence the apparent efficacy of these probes. For instance, 5×FAD mice develop dense and aggressive Aβ pathology by 2-3 months of age, providing a more robust imaging target, whereas APP/PS1 mice exhibit slower and more regionally restricted plaque development beginning around 5-6 months. These distinctions affect probe binding dynamics, fluorescence intensity, and temporal imaging windows, and should be considered when interpreting cross-study differences in diagnostic performance.

In relation to established clinical approaches, curcumin-based fluorescent probes offer several advantages over Food and Drug Administration (FDA)-approved Aβ PET tracers, such as florbetapir and flutemetamol. These include lower cost, absence of radioactivity, potential for real-time and longitudinal imaging, and even retinal-based detection. However, they are limited by shorter tissue penetration depth, formulation-dependent variability, rapid metabolism, and the lack of regulatory standardization. PET tracers benefit from validated pharmacokinetics, reproducibility, and broad clinical acceptance. Therefore, while curcumin probes show promise for early-stage or point-of-care diagnostics, their clinical utility will depend on further optimization, including enhancements in bioavailability, safety, and standardized imaging protocols.

Limitations: While curcumin-based fluorescent probes show considerable promise, a number of methodological and technical limitations inherent in the existing studies must be acknowledged. The included studies exhibited substantial methodological heterogeneity, including variations in probe structure, administration routes, imaging equipment, and animal models with differing Aβ pathology profiles. For instance, 5×FAD mice develop early and aggressive plaque accumulation, whereas APP/PS1 models display more gradual and regionally restricted pathology, complicating cross-study comparisons. Sample sizes were generally small, and few studies conducted direct, head-to-head comparisons under standardized conditions, limiting the ability to benchmark probe performance systematically. Moreover, long-term toxicity, biodistribution, and off-target accumulation were seldom evaluated, leaving gaps in the safety profile of these probes. Curcumin-based agents also face intrinsic technical challenges, such as photobleaching, poor aqueous solubility, rapid metabolic degradation, and formulation-dependent variability, all of which may compromise imaging consistency and translational reliability. These limitations highlight the need for further standardization and optimization to ensure the safe and effective clinical application of curcumin-based optical imaging strategies.

While risk of bias was assessed at the individual study level using the SYRCLE's Risk of Bias Tool, no formal assessment of reporting bias was performed at the synthesis level due to the descriptive, non-quantitative nature of this review. Likewise, the certainty of the evidence was not evaluated using formal frameworks such as GRADE. Finally, no review protocol was registered prior to the conduct of this systematic review, and therefore no protocol amendments were applicable.

Future directions and clinical translation: Although current evidence from preclinical studies is encouraging, the clinical applicability of curcumin-based fluorescent probes remains constrained by challenges such as rapid metabolism, limited solubility, and formulation variability. This review helps bridge the translational gap by identifying probes with favorable photophysical profiles and highlighting delivery strategies – such as polyethylene glycol (PEG) ylated micelles and liposomal systems – that enhance bioavailability and imaging performance. Importantly, our findings inform rational probe selection based on quantitative metrics (e.g., binding affinity, emission wavelengths, quantum yields) and model-dependent outcomes, which are critical for advancing in vivo imaging technologies.

In support of clinical relevance, multiple translational studies have demonstrated the feasibility of curcumin-based probes in human contexts. Liu et al. reported that a bivalent

curcumin-cholesterol ligand (BMAOI-14) crossed the BBB and specifically stained Aβ plaques in both Tg mouse models and human AD brain tissue.[15] More recently, An et al. developed a quinoline-curcumin-based probe [quinoline-derived half-curcumin-dioxaborine (Q-OB)] that sensitively detected Aβ oligomers in the cerebrospinal fluid (CSF) of patients with AD, distinguishing disease stages through fluorescence signal variation.[16] Complementing these findings, den Haan et al. showed that curcumin and its clinically bioavailable derivatives selectively bound fibrillar Aβ in post-mortem AD brains, with minimal cross-reactivity to other neurodegenerative pathologies.[17]

Collectively, these studies reinforce the translational promise of curcumin derivatives for in vivo diagnostics. Future directions include expanding cross-species validation, regulatory harmonization, and integration with artificial intelligence (AI)-assisted image analysis to optimize signal quantification and clinical applicability. These efforts will be critical for advancing curcumin-based probes toward safe and effective use in early AD detection.

Conclusion

Curcumin-based fluorescent probes show promise for preclinical applications in AD research, particularly due to their specificity for Aβ aggregates, potential for deep tissue imaging, and compatibility with non-invasive delivery methods. However, these findings are derived from heterogeneous preclinical studies with notable limitations, including variability in experimental protocols, probe formulations, and animal models, as well as limited assessment of long-term safety and clinical applicability. As such, while the reviewed evidence highlights their potential utility in early detection and disease monitoring, further standardized investigations – including validation in large animal or human models – are needed before these probes can be considered for clinical translation.

Conflict of Interests

The authors declare no conflict of interest in this study.

Acknowledgments

None.

References

1. Wu J, Shao C, Ye X, Di X, Li D, Zhao H, et al. InVivo Brain Imaging of Amyloid-β Aggregates in Alzheimer's Disease with a Near-Infrared Fluorescent Probe. ACS Sens 2021; 6(3): 863-70.
2. Fang D, Wen X, Wang Y, Sun Y, An R, Zhou Y, et al. Engineering of donor-acceptor-donor curcumin analogues as near-infrared fluorescent probes for in vivo imaging of amyloid-β species. Theranostics 2022; 12(7): 3178-95.
3. Sidiqi A, Wahl D, Lee S, Ma D, To E, Cui J, et al. In vivo Retinal Fluorescence Imaging with Curcumin in an Alzheimer Mouse Model. Front Neurosci 2020; 14: 713.
4. Khurshid B, Rehman AU, Muhammad S, Wadood A, Anwar J. Toward the Noninvasive Diagnosis of Alzheimer's Disease: Molecular Basis for the Specificity of Curcumin for Fibrillar Amyloid-β. ACS Omega 2022; 7(25): 22032-8.
5. Park YD, Kinger M, Min C, Lee SY, Byun Y, Park JW, et al. Synthesis and evaluation of curcumin-based near-infrared fluorescent probes for the in vivo optical imaging of amyloid-β plaques. Bioorg Chem 2021; 115: 105167.
6. Ni R, Villois A, Dean-Ben XL, Chen Z, Vaas M, Stavrakis S, et al. In-vitro and in-vivo characterization of CRANAD-2 for multi-spectral optoacoustic tomography and fluorescence imaging of amyloid-beta deposits in Alzheimer mice. Photoacoustics 2021; 23: 100285.
7. Si G, Zhou S, Xu G, Wang J, Wu B, Zhou S. A curcumin-based NIR fluorescence probe for detection of amyloid-beta (Aβ) plaques in Alzheimer's disease. Dyes Pigm 2019; 163: 509-15.
8. Ran C, Xu X, Raymond SB, Ferrara BJ, Neal K, Bacskai BJ, et al. Design, synthesis, and testing of difluoroboron-derivatized curcumins as near-infrared probes for in vivo detection of amyloid-beta deposits. J Am Chem Soc 2009; 131(42): 15257-61.
9. Chibhabha F, Yang Y, Ying K, Jia F, Zhang Q, Ullah S, et al. Non-invasive optical imaging of retinal Aβ plaques using curcumin loaded polymeric micelles in APP(swe)/PS1(ΔE9) transgenic mice for the diagnosis of Alzheimer's disease. J Mater Chem B 2020; 8(33): 7438-52.
10. Li Y, Yang J, Liu H, Yang J, Du L, Feng H, et al. Tuning the stereo-hindrance of a curcumin scaffold for the selective imaging of the soluble forms of amyloid beta species. Chem Sci 2017; 8(11): 7710-7.
11. Zhang X, Tian Y, Zhang C, Tian X, Ross AW, Moir RD, et al. Near-infrared fluorescence molecular imaging of amyloid beta species and monitoring therapy in animal models of Alzheimer's disease. Proc Natl Acad Sci U S A 2015; 112(31): 9734-9.
12. Zhang X, Tian Y, Li Z, Tian X, Sun H, Liu H, et al. Design and synthesis of curcumin analogues for in vivo fluorescence imaging and inhibiting copper-induced cross-linking of amyloid beta species in Alzheimer's disease. J Am Chem Soc 2013; 135(44): 16397-409.
13. Koronyo-Hamaoui M, Koronyo Y, Ljubimov AV, Miller CA, Ko MK, Black KL, et al. Identification of amyloid plaques in retinas from Alzheimer's patients and noninvasive in vivo optical imaging of retinal plaques in a mouse model. Neuroimage 2011; 54 Suppl 1: S204-17.
14. McClure R, Yanagisawa D, Stec D, Abdollahian D, Koktysh D, Xhillari D, et al. Inhalable curcumin: offering the potential for translation to imaging and treatment of Alzheimer's disease. J Alzheimers Dis 2015; 44(1): 283-95.
15. Liu K, Guo TL, Chojnacki J, Lee HG, Wang X, Siedlak SL, et al. Bivalent ligand containing curcumin and cholesterol as fluorescence probe for Aβ plaques in Alzheimer's disease. ACS Chem Neurosci 2012; 3(2): 141-6.
16. An J, Kim K, Lim HJ, Kim HY, Shin J, Park I, et al. Early onset diagnosis in Alzheimer's disease patients via amyloid-β oligomers-sensing probe in cerebrospinal fluid. Nat Commun 2024; 15(1): 1004.
17. den Haan J, Morrema THJ, Rozemuller AJ, Bouwman FH, Hoozemans JJM. Different curcumin forms selectively bind fibrillar amyloid beta in post mortem Alzheimer's disease brains: Implications for in-vivo diagnostics. Acta Neuropathol Commun 2018; 6(1): 75.